On the condensational growth of droplets in isotropic turbulence

On the condensational growth of droplets in isotropic turbulence

Michele Iovieno and Maurizio Carbone

Abstract The role of thermal inertia of droplets in the broadening of the droplet size distribution in homogeneous and isotropic turbulence is investigated. A new model for the condensational growth of water droplets, which takes into account the finite thermal relaxation time of droplets, is formulated. Results from direct numerical simulations with vanishing mean supersaturation in the two-way coupling regime show an increase of droplet size variance due to the increased fluctuations in the supersaturation field seen by each particle, which produce a differentiation of the growth conditions.

1 Introduction

Water droplets play a fundamental role in cloud dynamics, since the latent heat released or absorbed through water vapour condensation or evaporation is one of the main sources of energy which drives turbulent motions [1]. Since the paper by Vaillancourt et al. [2], direct numerical simulations have been used to study the small scale processes by numerically solving the interplay of small scale turbulent motions with phase transition processes. In these studies, the Eulerian description of the turbulent flow is coupled with the Lagrangian description of each individual droplet to investigate a small portion of a cloud. By simulating the evolution of droplets in a homogeneous and isotropic turbulent flow which resembles the well-mixed interior of a cloud, many works focused on how the local non-uniformity in the flow and in the droplet distribution can contribute to the broadening of the droplet

Michele Iovieno
Dipartimento di Ingegneria Meccanica e Aerospaziale, Politecnico di Torino, Corso Duca degli Abruzzi 24, 10129 Torino (Italy), e-mail: michele.iovieno@polito.it

Maurizio Carbone
Dipartimento di Ingegneria Meccanica e Aerospaziale, Politecnico di Torino, Corso Duca degli Abruzzi 24, 10129 Torino (Italy), e-mail: maurizio.carbone@polito.it

size distribution and therefore to the enhancement of their growth by collisions (e.g. [3, 4, 5]). Other studies have applied the same methodology to analyse interfacial phenomena where the mixing between supersaturared and undersaturated regions occurs, like the clear air entrainment at the lateral border (e.g. [6, 7, 8]) or at the border of a rising plume ([9, 10]). All these works use the model introduced by [2], who adapted the classical models for the condensational growth of a single droplet in quiescent, uniform environment [11]. In this model, thermal equilibrium between the droplet and the surrounding air is assumed: droplet temperature is determined by the instantaneous balance between the heat released by condensation and heat exchange with air. However, when the flow is turbulent the surrounding ambient seen by each droplet changes with a timescale dictated by small-scale turbulent eddies, so that local fluctuations of temperature and humidity occur on timescales which are of the same order of the droplet relaxation time. In these conditions, the finite thermal inertia of droplets cannot be neglected. Indeed, it has been shown that thermal inertia of particles plays an important role in the heat transport, since inertial particles in turbulent flows form clusters, which concentrate in the regions where the advected scalar fields display sharp gradients [12]. Thus, the droplets are strongly out of equilibrium with the surrounding fluid and large heat fluxes between fluid and particles would take place. In this work we reformulate the point mass model of droplets by considering a finite droplet thermal inertia. Results from simulations in forced and isotropic turbulence, with two-way coupling between the droplets and the fluid flow, are presented to assess the impact of the thermal inertia.

2 Model equations

Immediately following its formation through heterogeneous nucleation, a cloud droplet grows by vapour diffusion and condensation. Let us consider a droplet with radius R moving in humid air. Droplet radius is much smaller than the Kolmogorov microscale η and droplets are diluted, so that each droplet can be considered in a uniform environment. Since droplets are much denser than air and the Reynolds number of the relative motion of the particle in the surrounding air is small, droplets evolve subject to weight and Stokes drag,

$$\frac{\mathrm{d}\mathbf{x}}{\mathrm{d}t} = \mathbf{v}, \qquad \frac{\mathrm{d}\mathbf{v}}{\mathrm{d}t} = \frac{\mathbf{u}_\infty - \mathbf{v}}{\tau_u} + \mathbf{g}, \tag{1}$$

where $\mathbf{u}_\infty$ is the air velocity. Moreover, convection can be neglected and temperature T and vapour density ρ_v around a droplet are described by the Fourier equations,

$$\rho c_p \frac{\partial T}{\partial t} = \lambda \nabla^2 T, \qquad \frac{\partial \rho_v}{\partial t} = \kappa_v \nabla^2 \rho_v, \tag{2}$$

where ρ, c_p, and λ are the air density, specific heat at constant pressure and thermal conductivity, respectively, and κ_v is water vapour diffusivity, assumed constant since

T and ρ_v variations around the droplet are small. Analogously, the temperature in the spherical droplet is given by

$$\rho_L c_L \frac{\partial T}{\partial t} = \lambda_L \nabla^2 T \tag{3}$$

where ρ_L, c_L, and λ_L are the liquid water density, specific heat and thermal conductibility. Assuming spherical symmetry, all variables depend only on the radial coordinate r and the time t. The boundary conditions for $r \to +\infty$ are $T(r,t) \to T_\infty(t)$ and $\rho_v(r,t) \to \rho_{v,\infty}(t)$, which represent the matching with the surrounding ambient at $r \gg R$. At the droplet-humid air interface, $r = R(t)$, the continuity of temperature and of water mass flow imply that

$$\rho_L \frac{\mathrm{d}R}{\mathrm{d}t} = \kappa_v \frac{\partial \rho_v}{\partial r}(R^+, t), \qquad T(R^-, t) = T(R^+, t). \tag{4}$$

Moreover, the enthalpy variation due to condensation or evaporation should be equal to the net heat flow, obtaining a Stefan-like condition

$$-\rho_L L \frac{\mathrm{d}R}{\mathrm{d}t} = -\lambda_L \frac{\partial T}{\partial r}(R^-, t) + \lambda \frac{\partial T}{\partial r}(R^+, t) \tag{5}$$

where L is the latent heat of condensation. By integrating equation (3) in the droplet volume and using (4), equation (5) can be rewritten as

$$L\kappa_v \frac{\partial \rho_v}{\partial r}(R^+, t) = \frac{1}{R^2} \int_0^R \rho_L c_L \frac{\partial T}{\partial t} r^2 \mathrm{d}r - \lambda \frac{\partial T}{\partial r}(R^+, t). \tag{6}$$

Now, by considering that the diffusion timescales are much smaller than both the droplet growth timescale and the thermal relaxation timescale, the time derivatives into (2) and (3) can be neglected and a quasi-steady solution can be used, that is,

$$\rho_v(r,t) = \rho_{v,\infty} - (\rho_{v,\infty} - \rho_{vs}(T_d(t)) \frac{R(t)}{r} \tag{7}$$

$$T(r,t) = \begin{cases} T_d(t) & \text{if } r \le R(t) \\ T_\infty - (T_\infty - T_d(t)) \dfrac{R(t)}{r} & \text{if } r \ge R(t) \end{cases} \tag{8}$$

where $T_d(t)$ is the droplet surface temperature from (4). Introducing these solutions into (4) and (6), the following equations for the time evolution of the droplet radius and droplet temperature are obtained:

$$\frac{\mathrm{d}R}{\mathrm{d}t} = \frac{\kappa_v}{\rho_L} \frac{\rho_{v,\infty} - \rho_{vs}(T_d)}{R} \tag{9}$$

$$\frac{\mathrm{d}T_d}{\mathrm{d}t} = \frac{T_\infty - T_d}{\tau_\vartheta} + \frac{L\kappa_v}{\lambda} \frac{\rho_{v,\infty} - \rho_{vs}(T_d)}{\tau_\vartheta} \tag{10}$$

where $\tau_\vartheta = (\rho_L c_L R^2)/(3\lambda)$. When a set of N_d droplets moving in a turbulent flow is considered, $\mathbf{u}_\infty$, T_∞ and $\rho_{v,\infty}$ are the local velocity, temperature and vapour density in the fluid phase at each droplet position $\mathbf{x}_m$, that is $\mathbf{u}_\infty = \mathbf{u}(\mathbf{x}_m, t)$, $T_\infty = T(\mathbf{x}_m, t)$, $\rho_{v,\infty} = \rho_v(\mathbf{x}_m, t)$. In the absence of buoyancy, the flow is described by the incompressible Navier-Stokes equations, while temperature and water vapour are advected passive scalars,

$$\nabla \cdot \mathbf{u} = 0 \tag{11}$$

$$\frac{\partial \mathbf{u}}{\partial t} + \mathbf{u} \cdot \nabla \mathbf{u} = -\frac{1}{\rho_0}\nabla p + \nu \nabla^2 \mathbf{u} + \frac{1}{\rho_0}\mathbf{C}_u + \mathbf{f}_u \tag{12}$$

$$\frac{\partial T}{\partial t} + \mathbf{u} \cdot \nabla T = \kappa \nabla^2 T + \frac{1}{\rho_0 c_p} C_T + f_T \tag{13}$$

$$\frac{\partial \rho_v}{\partial t} + \mathbf{u} \cdot \nabla \rho_v = \kappa_v \nabla^2 \rho_v + C_d + f_v \tag{14}$$

where $\mathbf{f}_u$, f_T and f_v are external forcing terms and the source terms $\mathbf{C}_u$, C_T and C_d are the particle feedback terms, that is the momentum, enthalpy and water vapour transfer per unit volume and time from the droplets to the humid air phase. From equations (9) and (10), the feedback terms are given by

$$\mathbf{C}_u = \sum_{m=1}^{N_p} m_m \frac{\mathbf{v}_m(t) - \mathbf{u}(\mathbf{x}_m, t)}{\tau_{u,m}} \delta(\mathbf{x} - \mathbf{x}_m), \tag{15}$$

$$C_T = \sum_{m=1}^{N_p} c_L m_m \frac{T_{d,m}(t) - T(\mathbf{x}_m, t)}{\tau_{\vartheta,m}} \delta(\mathbf{x} - \mathbf{x}_m), \tag{16}$$

$$C_d = \sum_{m=1}^{N_p} 4\pi \kappa_v R_m^2 (\rho_{vs}(T_{d,m}(t)) - \rho_v(\mathbf{x}_m, t)) \delta(\mathbf{x} - \mathbf{x}_m). \tag{17}$$

where $m_m = 4\pi R_m^3/3$ is the mass of the m-th droplet and $\mathbf{v}_m$ its velocity.

3 Results and discussion

The evolution of initially monodisperse droplets with radius ranging from 15 to 25 μm in an isotropic turbulent flow with a Taylor microscale Reynolds number equal to 88 is investigated. Equations (9-10) and (11-14) are numerically solved in a triply periodic cubic domain by means of a 3/2 dealiased pseudo-spectral spatial discretization, a second order exponential time integrator and fourth order spline interpolation/reconstruction for the coupling terms [13]. Deterministic large-scale forcing is implemented to maintain a constant dissipation rate $\varepsilon = 5 \cdot 10^{-3}$ m^2/s^3, typical of warm clouds, and a variance of temperature and vapour density equal to 0.25% their mean values. The reference mean temperature is $T_0 = 280$ K and the mean vapour density is chosen so that the mean supersaturation is equal to zero

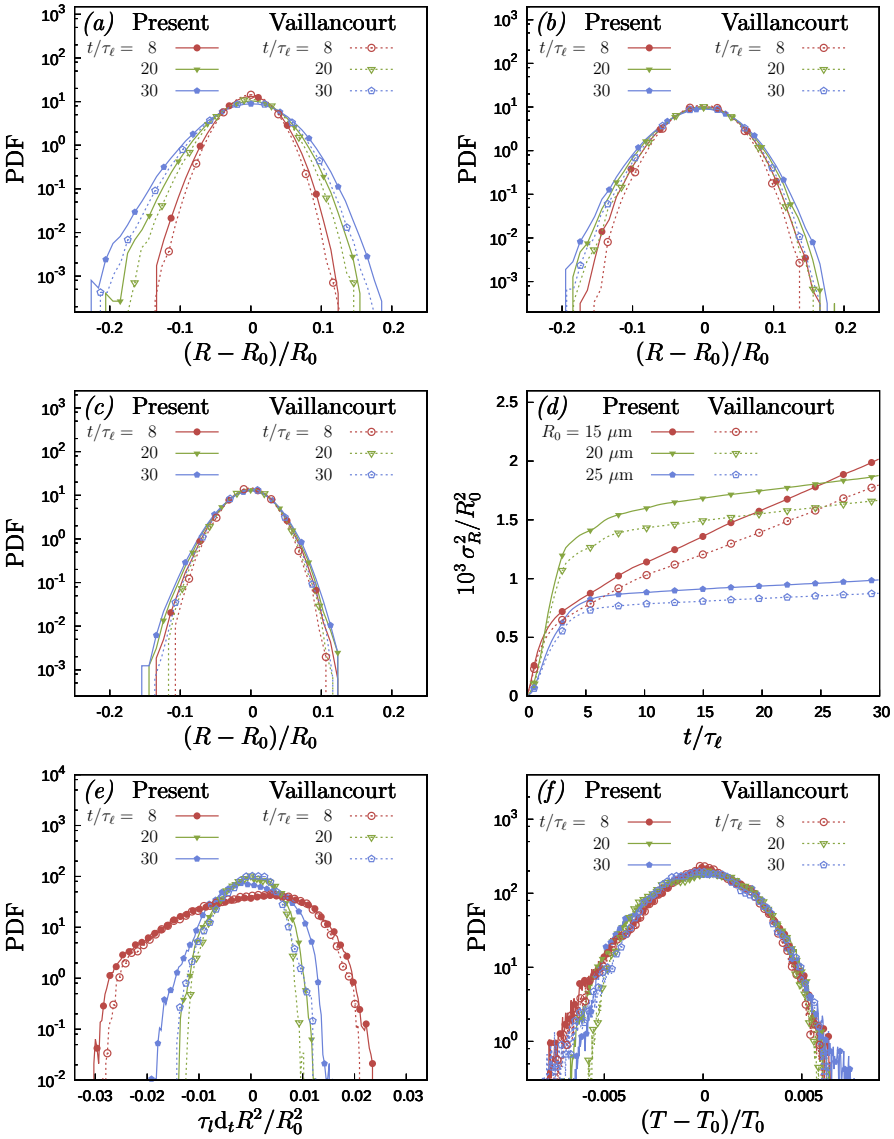

Fig. 1 Probability density functions (PDF) of the droplet relative size variation $(R - R_0)/R_0$, at different times, for droplet initial radius $R_0 = 15\mu$m *(a)*, 20μm *(b)* and *(c)* 25μm. *(d)* Time evolution of the droplet radius variance. PDF of the dimensionless particle radius rate of change *(e)* and of the particle temperature fluctuations for $R_0 = 20\mu$m *(f)*. Time is rescaled with the integral timescale $\tau_\ell = \ell/u'$, where ℓ is the integral scale and u' the root mean square of velocity fluctuations.

$(\langle\rho_v\rangle = \rho_{vs}(T_0))$ as in [3], so that there is no mean growth. With this set of parameters, Kolmogorov microscale η is equal to 1 mm, Kolmogorov timescale τ_η is 0.05 s, the Stokes number τ_u/τ_η ranges from 0.06 to 0.16 and the thermal Stokes number τ_ϑ/τ_η

from 0.25 to 0.7. Droplet volume fraction is kept equal to 10^{-6} in all simulations. Figures 1 *(a-c)* show the probability density function (PDF) of the droplet radii at different times and for various initial radii R_0. The inclusion of thermal inertia widens the tails and produces a larger variance of R, as in Figure 1 *(d)*. The variance of the size of the smallest droplets tends to grow as $t^{1/2}$ while larger droplets grow slower. The novel model here proposed, which includes thermal inertia, always predicts a faster droplet growth than the classic model [2]: a 10% larger variance is obtained after a minute and the difference between the variances grows in time. Small droplets grow or shrink faster than large droplets because of the R^{-1} factor in (9). On the other hand, large droplets experience larger supersaturation variations since they are affected by their path history. These two concurrent effects, when the variance of the fields is imposed, lead to a non-monotonic dependence of the droplet size variance on the droplet initial radius. The broadening due to the particle inertia increases with the Stokes number, since the temperature differences experienced by the droplets increase. Thus, the growth due to the lack of thermal equilibrium can be expected to be particularly significant in the cloud regions with locally higher dissipation rates, leading to a local broadening of size distribution which can accelerate the collisional growth. Moreover, the broadening is also enhanced by the intermittency of the vapour density and temperature fields which increases with the Reynolds number.

Acknowledgements We acknowledge the CINECA award under the ISCRA initiative, for the availability of high performance computing resources (project HP10CEG6MK).

References

1. Devenish, B.J., et al.: Quart. J. Roy. Meteor. Soc., **138**, 1401–1429, (2012).
2. Vaillancourt, P.A., Yau, M.K., Grabonski, W.W.: J. Atmos. Sci., **58**, 1945–1964, (2001).
3. Lanotte, A., Seminara A., Toschi, F.: J. Atmos. Sci. **66**, 1685–1697, (2009).
4. Sardina, G., Picano, F., Brandt, L., Caballero, R.: Phys. Rev. Lett. **115**, 184 501, (2015).
5. Gotoh, T., Suchito T., Saito I.: New J. Phys, **19**, 043 042, (2016).
6. Kumar, B., Janetzko F., Schumacher J., Shaw, R.A.: New J. Phys., **14**, 115020, (2012).
7. Kumar, B., Schumacher, J., Shaw, R.A.: Theor. Comput. Fluid Dyn. **27**, 361–376, (2013).
8. Kumar, B., Schumacher, J., Shaw, R.A.: J. Atmos. Sci. **71**, 2564–2580, (2014).
9. Perrin, V.E., Jonker, H.J.: J. Atmos. Sci., **72**, 4015–4028, (2015).
10. Götzfried, P., Kumar, B., Shaw, R.A., Schumacher, J.: J. Fluid Mech. **814**, 452–483, (2017).
11. Pruppacher, H.R., Klett J.D.: Microphysics of Clouds and Precipitation,Springer, (2010).
12. Bec, J., Homann, H., Bay, S.S.: phys. Rev. Lett. **112**, 184 501, (2014).
13. Carbone, M., Iovieno, M.: WIT Trans. Eng. Sci. **120**, 237–248, (2018).